

Global acceleration in rates of vegetation change over the past 18,000 years

Ondřej Mottl^{1*†}, Suzette G.A. Flantua^{2*†}, Kuber P. Bhatta¹, Vivian A. Felde², Thomas Giesecke³, Simon Goring^{4,5}, Eric C. Grimm^{6‡}, Simon Haberle^{7,8}, Henry Hooghiemstra⁹, Sarah Ivory¹⁰, Petr Kuneš¹¹, Steffen Wolters¹², Alistair W. R. Seddon², John W. Williams^{4,5}

Affiliations

1. Department of Biological Sciences, University of Bergen, PO Box 7803, N-5020 Bergen, Norway

2. Department of Biological Sciences and Bjerknes Centre for Climate Research, University of Bergen, PO Box 7803, N-5020 Bergen, Norway.

3. Department of Physical Geography, Utrecht University, P.O. Box 80115, 3508 TC Utrecht, The Netherlands.

4. Department of Geography, University of Wisconsin-Madison, Madison, WI, USA

5. Center for Climatic Research, University of Wisconsin-Madison, Madison, WI, USA

6. Department of Earth and Environmental Sciences, University of Minnesota, Minneapolis, Minnesota 55455, USA

7. Department of Archaeology and Natural History, Australian National University, Canberra, ACT 2601, Australia.

8. Australian Research Council Centre of Excellence in Australian Biodiversity and Heritage, Australian National University, Canberra, ACT 2601, Australia

9. Department of Ecosystem and Landscape Dynamics, University of Amsterdam, Science Park 904, 1098 XH, Amsterdam, the Netherlands

10. Department of Geosciences and the Earth and Environmental Systems Institute (EESI), Penn State University, University Park, PA 16801, USA

11. Department of Botany, Faculty of Science, Charles University, Czech Republic

27 12. Lower Saxony Institute for Historical Coastal Research, Wilhelmshaven, Germany.

28 †Equal contribution. ‡ Deceased.

29

30 *Corresponding authors: Ondrej Mottl (ondrej.mottl@gmail.com), Suzette Flantua

31 (s.g.a.flantua@gmail.com)

32

33 **One sentence summary:** A compilation of over 1000 fossil pollen sequences shows that global
34 vegetation change accelerated several thousand years ago.

35

36 **Abstract**

37 Global vegetation over the last 18,000 years was transformed first by the climate changes
38 accompanying the last deglaciation and again by increasing human pressures, but the magnitude and
39 patterns of rates of vegetation change are poorly understood globally. Using a compilation of 1181
40 fossil pollen sequences and new statistical methods, we detect a worldwide acceleration in rates of
41 vegetation compositional change beginning between 4.6 and 2.9 ka that is globally unprecedented over
42 the last 18,000 years in magnitude and extent. Late Holocene rates of change equal or exceed deglacial
43 rates for all continents, suggesting that the scale of human impacts on terrestrial ecosystems exceeds
44 even the climate-driven transformations of the last deglaciation. The acceleration of biodiversity
45 change demonstrated in last-century ecological datasets began millennia ago.

46

47 **Main text**

48 One of the clearest forms of biodiversity change during the past century has been the increased rates of
49 species turnover across the marine and terrestrial biosphere (1–3). Today, over 75% of the Earth’s ice-
50 free land surface has been altered by human land use (4), with profound effects on the composition
51 and functioning of ecosystems. Globally, extinction rates are increasing (5), although trends in local
52 species richness are ambiguous (6).

53 These increased rates of species turnover, as signified by local and regional changes in
54 community composition, are embedded within a longer-term context in which humanity’s footprint

55 has steadily grown since humans first began to alter landscapes for food, energy, and other resources.
56 Hominid use of fire began at least 700,000 years ago (7), low-intensity but extensive agricultural land
57 use began ca. 8000 years ago, while intensive agricultural land use expanded after 6000 years ago (8)
58 (**Fig. 1B**). Detectable human imprints on vegetation began thousands of years ago (e.g. 9, 10), and the
59 composition and carbon sequestration of many contemporary ecosystems remain profoundly
60 influenced by legacies of past centuries to millennia of anthropogenic land use (e.g. 11). Nonetheless,
61 there remains a major knowledge and scale gap between contemporary studies of global biodiversity
62 trends of the last century (2) and studies examining early anthropogenic effects on ecosystems.
63 Observational syntheses of global biodiversity trends are limited to the past several centuries, while
64 macroscale syntheses of vegetation changes from fossil pollen data have been limited to continental
65 scales (e.g. 9) or are largely qualitative (e.g. 12). Consequently, global patterns and magnitudes of
66 vegetation compositional change, which are important for understanding how biodiversity and
67 ecosystem dynamics have been shaped by climate change and early human activity, are poorly
68 understood.

69 In parallel, paleoecological studies have shown the high sensitivity of terrestrial ecosystems to
70 the climate changes accompanying and following the last deglaciation (ca. 20,000 to 8200 cal yr BP;
71 20 to 8.2 ka, **Figs. 1C,D**) (12, 13). In temperate and boreal regions, forest expanded from glacial
72 refugia as temperatures rose and precipitation patterns shifted, with widespread leading-edge range
73 expansions and, for some taxa, trailing-edge range contractions (14). Novel ecosystems emerged in
74 response to novel climates and the late Pleistocene extinction of megaherbivores (15). Tropical and
75 subtropical ecosystems responded to rising temperatures linked to increasing greenhouse gases (**Fig.**
76 **1D**) and hydrological shifts driven by precessional controls on monsoons and the Intertropical
77 Convergence Zone (16). Consequently, during the Pleistocene-Holocene transition, tropical
78 ecosystems substantially changed in species composition and canopy structures across all elevations
79 (17), while millennial- and centennial-scale hydroclimate variability caused abrupt changes in global
80 vegetation during the Holocene (18).

81 Ecosystem responses to humans and climate change over long timescales can now be assessed
82 globally, thanks to the century-long expansion of a global network of fossil pollen sequences anchored

83 by increasingly precise radiocarbon chronologies (e.g. 19), the building of open, community-curated
84 data resources (20), and the development of new rate-of-change techniques (21). Here, we assess the
85 global patterns and rates of vegetation change from the last deglaciation, through the Holocene and up
86 to the current Anthropocene, based on 1181 fossil pollen sequences from the Neotoma Paleoecology
87 Database (20) covering all continents except Antarctica (**Fig. 1, Data S1**). These analyses are based on
88 continentally harmonized taxonomies and updated Bayesian chronologies with age-depth model
89 uncertainties and an improved algorithm (R package *R-Ratepol*; 21, 22) for estimating Rates of
90 Change (RoC) for paleoecological time series. RoCs are calculated as the compositional dissimilarity
91 between consecutive time intervals (using the chi-squared coefficient) standardized by the length of
92 time between samples, therefore providing an indicator of compositional change per unit time. *R-*
93 *Ratepol* uses a moving-window approach (instead of the traditional calculation of dissimilarities
94 between individual levels), which minimizes artifactual alterations in RoC due to variations in sample
95 density and sedimentation rate (21). *R-Ratepol* also incorporates temporal uncertainty resulting from
96 age-depth modelling calculations via randomization (21, 22). For each pollen sequence, we pooled
97 data into 500-yr time bins (see also our 250-yr sensitivity experiment in SM (22)) and calculated RoC
98 between bins to represent rate of compositional change through time. For each sequence, we also
99 identified time intervals with a large increase in rate of change, called ‘peak points’ (for more detailed
100 information see methods in SM (22)).

101 We analyze RoCs at the scale of continents and sub-continental clusters, defined by climatic
102 and geographic variables (22). For each continent and sub-continental region, we binned the RoC
103 scores per 500-yr time bins (with a 250-yr sensitivity experiment in SM (22)) and calculated the 95%
104 RoC quantile to highlight intervals and places with large vegetation changes while filtering out outliers
105 (see 22 for a comparison of the 95% quantile to median trends). Similarly, we calculated the
106 proportion of sequences with a peak point in each time bin. The clustering of peak points among
107 sequences indicates a synchronous period of abrupt vegetation change within a region. Generalized
108 Additive Models (GAMs) were fitted to all RoC and peak point curves to summarize trends and test
109 for significant accelerations (simultaneous confidence intervals of the first derivative differ from zero,
110 22).

111 We detect an unequivocal global acceleration of vegetation change during the late Holocene
112 (4.2–0 ka; **Fig. 2**). The estimated start of acceleration differs among continents and ranges from 4.6 to
113 3.1 ka (**Table S1**). This estimated start is well supported by the dense availability of samples during
114 the middle to late Holocene (**Fig. 1E**), but continental-scale estimates vary by ca. 500-1000 years (22).
115 For most continents, late Holocene RoCs are close to or exceed RoCs over the last 18 ka, with a
116 percent differential ranging from -6.3% to 22.2 % (**Fig. 2, Table S1**). Increases in RoC during the
117 Lateglacial and early Holocene can be linked to temperature and atmospheric CO₂ variations (**Figs.**
118 **1C,D**) and to hydrological variations. Rapid vegetation changes concentrate near to the onset of the
119 Holocene (11.7 ka) for most continents, expressed as a maximum in RoC or in peak points (**Fig. 2**). In
120 North America and Europe, RoCs reached maxima during the abrupt millennial-scale climate
121 oscillations characteristic of the North Atlantic and adjacent regions (ca. 15 to 11 ka), then
122 substantially declined during the early Holocene (**Fig. 2A, B**). The heightened rates of deglacial
123 vegetation change resembles the patterns of increased temperature variability in the North Atlantic and
124 elsewhere in the Northern Hemisphere that were driven by a combination of orbital forcing,
125 atmospheric greenhouse gas concentrations, meltwater pulses to the North Atlantic, and shifting
126 patterns of heat transport (23). In Asia, rapid but asynchronous change characterizes the Lateglacial
127 and deglaciation period, with a maximum in RoCs or a clustering of peak points between 10 and 8 ka
128 (**Fig. 2C**). In Latin America and Africa, RoCs also reach maxima between 10 and 8 ka, which can be
129 linked to altered monsoonal rainfall associated with declining Northern Hemisphere summer
130 insolation (24).

131 RoC patterns at subcontinental scales are consistent with known histories of climate change
132 and human land use. For example, in Eurasia, the western and northern European clusters show strong
133 peaks in the rate of vegetation change between 15 and 10 ka (**Figs. 3A,E**), consistent with the response
134 of vegetation to North Atlantic climate variations and the retreating Eurasian ice sheets (**Fig. 1C**). Late
135 Holocene rates of vegetation change are high across western and central Europe and particularly in
136 areas of high present and past agricultural activity (10). In Asia, high rates of vegetation change during
137 the early Holocene can be linked to post-glacial forest expansion in northern Asia (25) and to

138 millennial-scale variability in temperature and monsoonal rainfall in eastern Asia (26) (**Figs. 3C,D,I**).
139 Seven of ten Eurasian clusters show increased RoCs during the late Holocene.

140 In the Americas, vegetation RoCs vary by latitude and between Atlantic- and Pacific-adjacent
141 regions (**Fig. 4**). Eastern North America resembles western Europe in its high vegetation RoCs
142 between 15 and 10 ka, with a strong signal of synchronous vegetation change over the last millennium
143 (**Fig. 4G,H,I**). All North American regions show increased RoCs during the late Holocene except for
144 the high-latitude clusters. Driven by the topographic complexity of the Andes, vegetation responses in
145 the Neotropical highlands were highly variable and asynchronous (**Fig. 4D**) likely a combined effect
146 of changes in temperature, hydroclimate variability and atmospheric CO₂ (27, 28). In the lowlands, a
147 peak in vegetation RoCs at 10 ka is likely due to hydrological variability linked to shifting monsoons
148 (**Fig. 4J**) (27). These large vegetation changes challenge the common myth of the ‘stable’ tropics and
149 suggest a strong sensitivity of the Neotropics to temperature, hydroclimate variability and orbital
150 precession during the early Holocene (27, 28). In temperate South America, a period of synchronous
151 vegetation change in the Holocene (**Fig. 4E**) is asynchronous with warm Neotropical regions (**Fig.**
152 **4J**), likely due to varying climate modes influencing different parts of the continent (29). The late
153 Holocene acceleration of vegetation change is clearly manifested across most of the latitudinal
154 gradient of the Americas, except for the high northern latitudes, with the highest RoCs in coastal
155 western North America and eastern North America (**Fig. 4**).

156 The detection of globally accelerating rates of vegetation change during the late Holocene
157 provides a longer-term perspective to the well-documented increase in species turnover during the 20th
158 and 21st century (6). For terrestrial ecosystems at least, these recent increases in species turnover are
159 the continuation of a longer acceleration that began millennia ago (**Fig. 2**). Moreover, this work
160 suggests that contemporary communities and some current biodiversity trends may be partially due to
161 legacies of past land use or environmental forcing (11) in combination with the strong anthropogenic
162 imprint of the last decades. Hence, recent changes in biodiversity patterns represent only the most
163 recent interval of our used planet (30) that has been altered by millennia of changing environments and
164 human activities.

165 Our study has focused primarily on detecting patterns of rates of vegetation compositional
166 changes over the last 18,000 years and secondarily on attributing causes. This approach follows the
167 standard delineation in climate change research between detection studies that focus on establishing
168 the significance and fingerprints of observed climate trends (31) and attribution studies that explore
169 the potential causes of the observed events and patterns (32). Biodiversity research is now achieving
170 the capability for global detection analyses (2, 6) across an increasingly broad range of timescales. The
171 next major frontier is to disentangle and attribute the contributions of climatic variability and
172 anthropogenic impacts to past vegetation changes. This attribution is challenged by the complex
173 interplay among climatic, anthropogenic, and vegetation dynamics that varies within and among
174 ecosystems, particularly at local to regional scales. For instance, in the Holocene in East Africa, land
175 cover changes over the last 6000 years were driven by multiple cultural and technological innovations
176 and by changes in rainfall amount and seasonality (33). In South America, Holocene climate
177 variability contributed to regime shifts in human demography and displacement, which in turn affected
178 ecosystems regionally (34). The worldwide spread of agricultural land-use over the last 3000 years
179 suggests intensified resource management (8), but was accompanied in some regions by significant
180 climate changes (16, 33). Deglacial vegetation dynamics, although strongly climate-driven, were also
181 affected by global megaherbivore extinctions during the late Quaternary (15), that likely resulted from
182 synergistic anthropogenic and climatic drivers (35). These interactions argue against single-cause
183 attributions of rates of vegetation change.

184 A key next step is to integrate these paleovegetation sequences with other paleoclimatic and
185 archaeological records in order to better understand the past feedbacks among climate, ecosystems,
186 and humans (3, 10, 13, 36), and the legacy effects of these past interactions on the trajectory of
187 contemporary ecosystems. Assembled networks of paleovegetation, paleoclimatic, and anthropogenic
188 records need to be harmonized and quality checked in order to do this attribution correctly and handle
189 the spatial variations in vegetation, climate, and human histories within and among continents (e.g.
190 36). Such an integration will also need carefully chosen numerical techniques to formally detect the
191 onset of detectable human influence in paleoenvironmental time series and the variation in timing

192 within and among ecosystems (29). Additionally, a higher density of paleoecological records is still
193 critically needed, especially in topographically rich regions such as the Himalayas and the Andes
194 where climate heterogeneity is highest and human activities span millennia.

195 Despite these complexities, it is well known that the mean global temperature increases during
196 the last deglaciation (ca. 6°C) were several times larger than those of the middle to late Holocene (ca.
197 1°C, 37). Hence, a reasonable working inference is that the globally enhanced rates of vegetation
198 change over the last several thousand years were caused primarily by anthropogenic activities, while
199 vegetation changes during the late Pleistocene to early Holocene were driven primarily by changing
200 climates. If so, the magnitude and extent of late Holocene rates of vegetation change suggests that the
201 global transformation of the terrestrial biosphere by humans now resembles or exceeds in rate and
202 scope even the profound ecosystem transitions associated with the end of the last glacial period.
203 Moreover, the global ecosystem changes for this century may be greater yet, given current climate
204 commitments and given that the climate changes expected for higher-end emission scenarios are
205 similar in magnitude to those of the last deglaciation.

206

207 **References and notes**

- 208 1. B. J. McGill, M. Dornelas, N. J. Gotelli, A. E. Magurran, *Trends Ecol. Evol.* 30, 104–113 (2015).
- 209 2. M. Dornelas et al., *Glob. Ecol. Biogeogr.* 27, 760–786 (2018).
- 210 3. J. Woodbridge et al., *J. Ecol.* 109, 1396–1410 (2021).
- 211 4. E. C. Ellis, N. Ramankutty, *Front. Ecol. Environ.* 6, 439–447 (2008).
- 212 5. S. L. Pimm et al., *Science* 344, 1246752 (2014).
- 213 6. S. A. Blowes et al., *Science* 366, 339–345 (2019).
- 214 7. D. M. J. S. Bowman et al., *J. Biogeogr.* 38, 2223–2236 (2011).
- 215 8. L. Stephens et al., *Science* 365, 897–902 (2019).
- 216 9. T. Giesecke et al., *Nat. Commun.* 10, 5422 (2019).
- 217 10. L. Marquer et al., *Quat. Sci. Rev.* 171, 20–37 (2017).
- 218 11. C. N. H. McMichael, *New Phytol.* 229, 2492–2496 (2021).
- 219 12. C. Nolan et al., *Science* 361, 920–923 (2018).
- 220 13. D. A. Fordham et al., *Science* 369, eabc5654 (2020).
- 221 14. J. W. Williams, B. N. Shuman, T. Webb III, P. J. Bartlein, P. L. Leduc, *Ecol. Monogr.* 74, 309–
- 222 334 (2004).
- 223 15. Y. Malhi et al., *Proc. Natl. Acad. Sci. U.S.A.* 113, 838–846 (2016).
- 224 16. F. E. Mayle, D. J. Beerling, W. D. Gosling, M. B. Bush, *Phil. Trans. R. Soc. Lond. B* 359, 499–
- 225 514 (2004).
- 226 17. F. E. Mayle, M. J. Burn, M. Power, D. H. Urrego, in *Past Climate Variability in South America*
- 227 *and Surrounding Regions*,
- 228 F. Vimeux, F. Sylvestre, M. Khodri, Eds., vol. 14 of *Developments in Paleoenvironmental Research*
- 229 (Springer, 2009), pp. 89–112.
- 230 18. A. W. Seddon, M. Macias-Fauria, K. J. Willis, *Holocene* 25, 25–36 (2015).
- 231 19. S. G. A. Flantua et al., *Rev. Palaeobot. Palynol.* 223, 104–115 (2015).
- 232 20. J. W. Williams et al., *Quat. Res.* 89, 156–177 (2018).
- 233 21. O. Mottl et al., bioRxiv 2020.12.16.422943 [Preprint].
- 234 24 February 2021. <https://doi.org/10.1101/2020.12.16.422943>.
- 235 22. See supplementary materials online.
- 236 23. Z. Liu et al., *Science* 325, 310–314 (2009).
- 237 24. T. M. Shanahan et al., *Nat. Geosci.* 8, 140–144 (2015).
- 238 25. G. M. MacDonald, K. V. Kremenetski, D. W. Beilman, *Phil. Trans. R. Soc. B* 363, 2283–2299
- 239 (2008).
- 240 26. H. Zhang et al., *Quaternary* 2, 26 (2019).

241 27. V. F. Novello et al., *Earth Planet. Sci. Lett.* 524, 115717 (2019).

242 28. M. H. M. Groot et al., *Clim. Past* 7, 299–316 (2011).

243 29. S. G. A. Flantua et al., *Clim. Past* 12, 483–523 (2016).

244 30. E. C. Ellis et al., *Proc. Natl. Acad. Sci. U.S.A.* 110, 7978–7985 (2013).

245 31. PAGES 2k Consortium, *Nat. Geosci.* 6, 339–346 (2013).

246 32. K. E. Trenberth, J. T. Fasullo, T. G. Shepherd, *Nat. Clim. Chang.* 5, 725–730 (2015).

247 33. R. Marchant et al., *Earth Sci. Rev.* 178, 322–378 (2018).

248 34. P. Riris, M. Arroyo-Kalin, *Sci. Rep.* 9, 6850 (2019).

249 35. E. D. Lorenzen et al., *Nature* 479, 359–364 (2011).

250 36. A. Bevan et al., *Proc. Natl. Acad. Sci. U.S.A.* 114, E10524–E10531 (2017).

251 37. J. E. Tierney et al., *Nature* 584, 569–573 (2020).

252 38. North Greenland Ice Core Project members, *Nature* 431, 147–151 (2004).

253 39. E. Monnin et al., *Science* 291, 112–114 (2001).

254 40. O. Mottl, S. Flantua, HOPE-UIB-BIO/Global_RoC: First public release, version v1.0, Zenodo
255 (2021); <http://doi.org/10.5281/zenodo.4650239>.

256 41. S. G. A. Flantua et al., “Mottl et al. (2021, Science) Taxonomic harmonization tables for North
257 America, Latin America, Europe, Asia, Africa,” Figshare, dataset (2021);
258 <https://doi.org/10.6084/m9.figshare.13049735>.

259

260 **Acknowledgements:** We are grateful to all data contributors to Neotoma and data stewards for
261 constituent databases of African Pollen Database, European Pollen Database, IndoPacific
262 Palaeoecology Database, Latin American Pollen Database, and North American Pollen Database, for
263 supporting open-access data. We thank H. John B. Birks for suggestions to the analyses and for
264 providing advice on the Asian taxonomic harmonization. **Funding:** O.M., S.G.A.F., K.P.B., V.A.F.
265 and A.W.R.S. acknowledge support from the European Research Council (ERC) under the European
266 Union’s Horizon 2020 research and innovation programme (grant agreement No 741413) to H. John
267 B. Birks. Neotoma development has been supported by the National Science Foundation (1550707,
268 1550805, 1948926) and Belmont Forum (1929476). **Author contributions:** O.M., S.G.A.F.,
269 A.W.R.S., J.W.W. designed the study. S.G.A.F., K.P.B., V.A.F., A.W.R.S. and O.M. developed the
270 data extraction workflow and O.M. performed the numerical analyses. J.W.W., H.H., S.G.A.F., K.P.B.
271 and S.I led the compilation and taxonomic harmonization of continental-scale pollen datasets. E.C.G,

272 T.G., S.H., H.H., S.I., S.G.A.F, and J.W.W. led Neotoma data mobilization efforts. S.G.A.F. and
273 J.W.W. lead the writing. All authors contributed to the article and approved the submitted version.
274 **Competing interests.** The authors declare no competing interests. **Data and materials availability:**
275 All the data and R codes are publicly available at Zenodo (40) and at <https://github.com/HOPE-UIB->
276 [BIO/Global_RoC](#). Harmonization tables are available at Figshare (41).

277

278 **SUPPLEMENTARY MATERIALS**

279 Materials and Methods

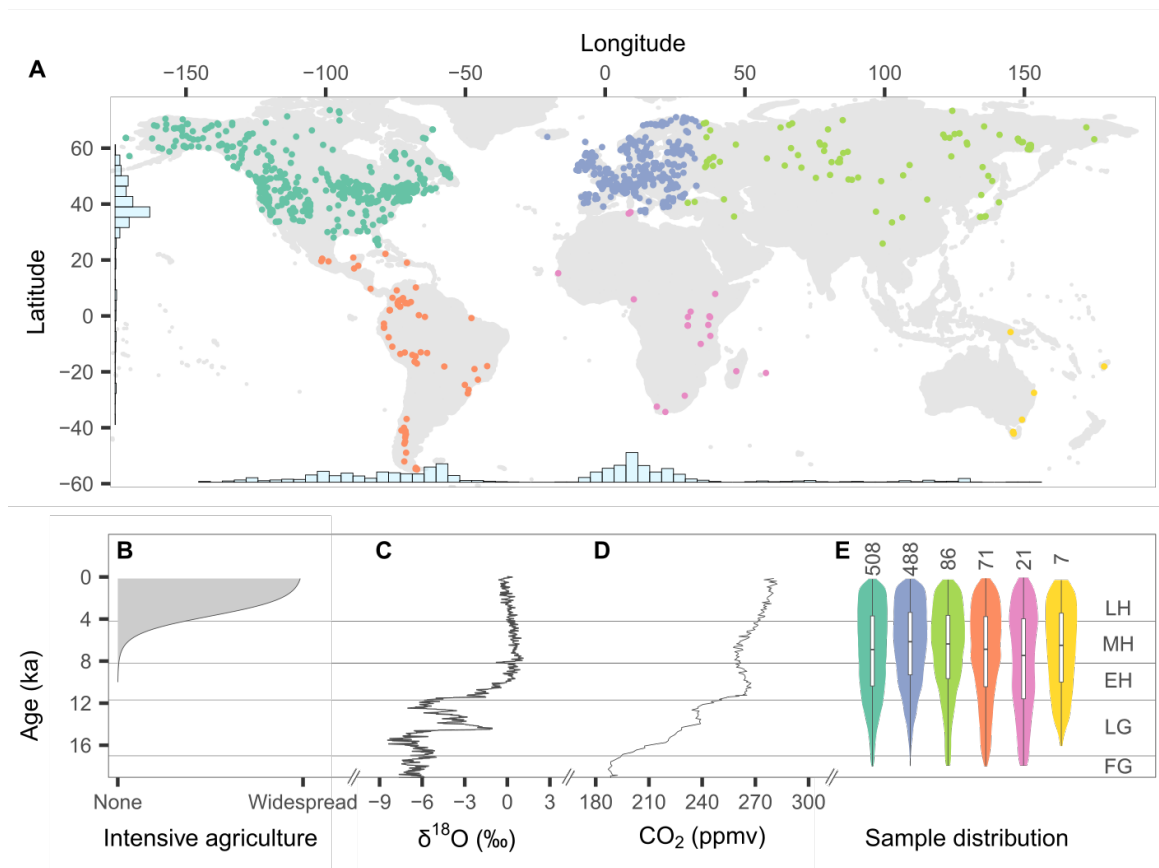
280 Figs. S1-S7

281 Tables S1-S3

282 References (42-77)

283 Data S1

284



286

287 **Figure 1 | Spatiotemporal distribution of the fossil pollen sequences analyzed here and climate**

288 **and anthropogenic changes during the last 18.000 yr. A) Spatial distribution of used pollen**

289 sequences. Histograms indicate the frequency of sequences across longitude and latitude. B)

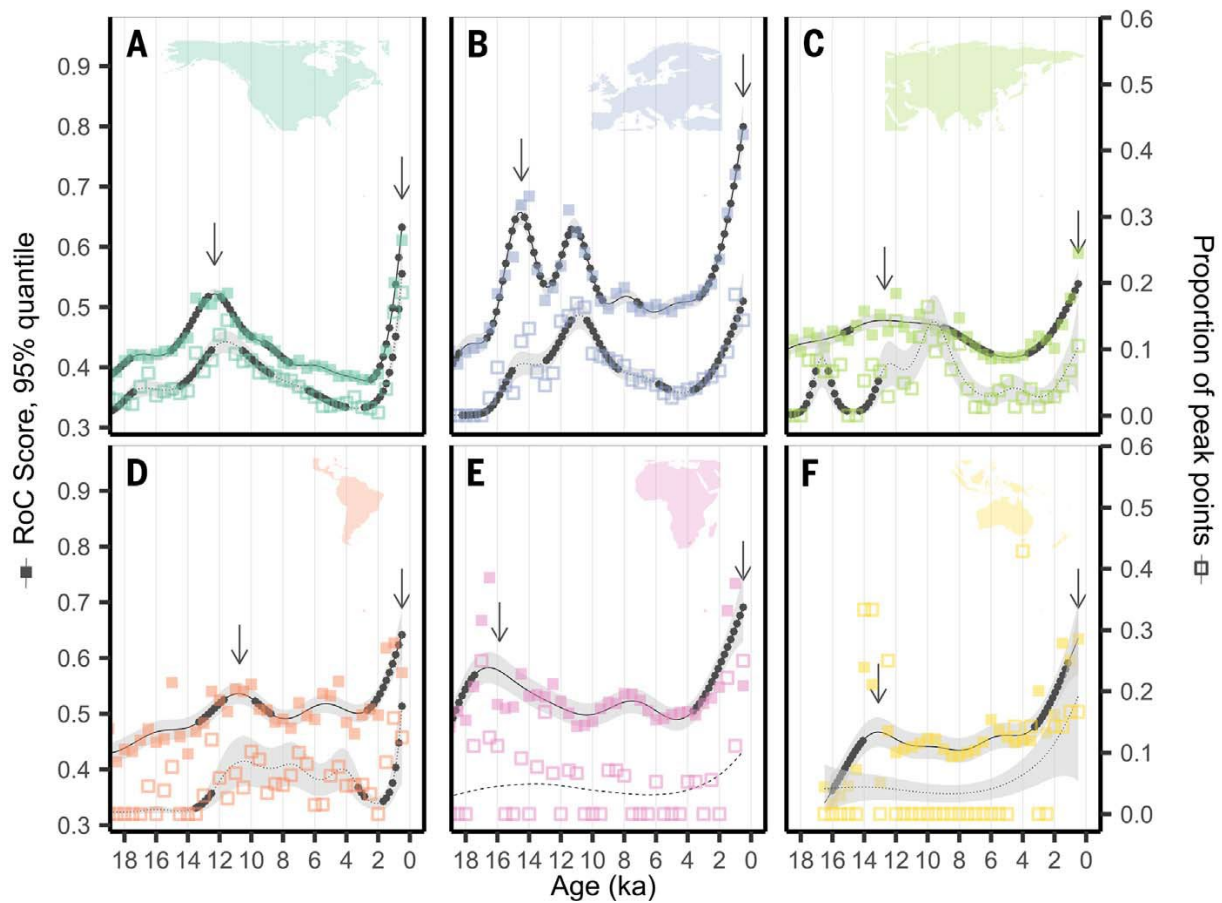
290 Development of intensive agriculture based on archaeological expert elicitation (8). C) $\delta^{18}\text{O}$, a

291 temperature proxy, from the North Greenland Ice Core Project (NGRIP) (38). D) Atmospheric CO_2

292 concentration (ppmv; EPICA DOME C, 39). E). The number of pollen sequences per continent (colors

293 match panel A) and sample density over the studied period. FG: Full Glacial; LG: Lateglacial; EH:

294 Early Holocene, MH: Middle Holocene, LH: Late Holocene.



296

297 **Figure 2 | Rate of Change (RoC) analyses by continent.** The filled squares represent the upper 95%

298 quantile RoC score (left y-axis) per 500 yr time bin with the solid curve representing the

299 corresponding generalized additive model (GAM, 22). High values indicate high rates of vegetation

300 change. Empty squares represent the proportion of peak points within each time bin (right y-axis) with

301 the corresponding GAM curve (dotted line). High values indicate a high synchrony in RoC among

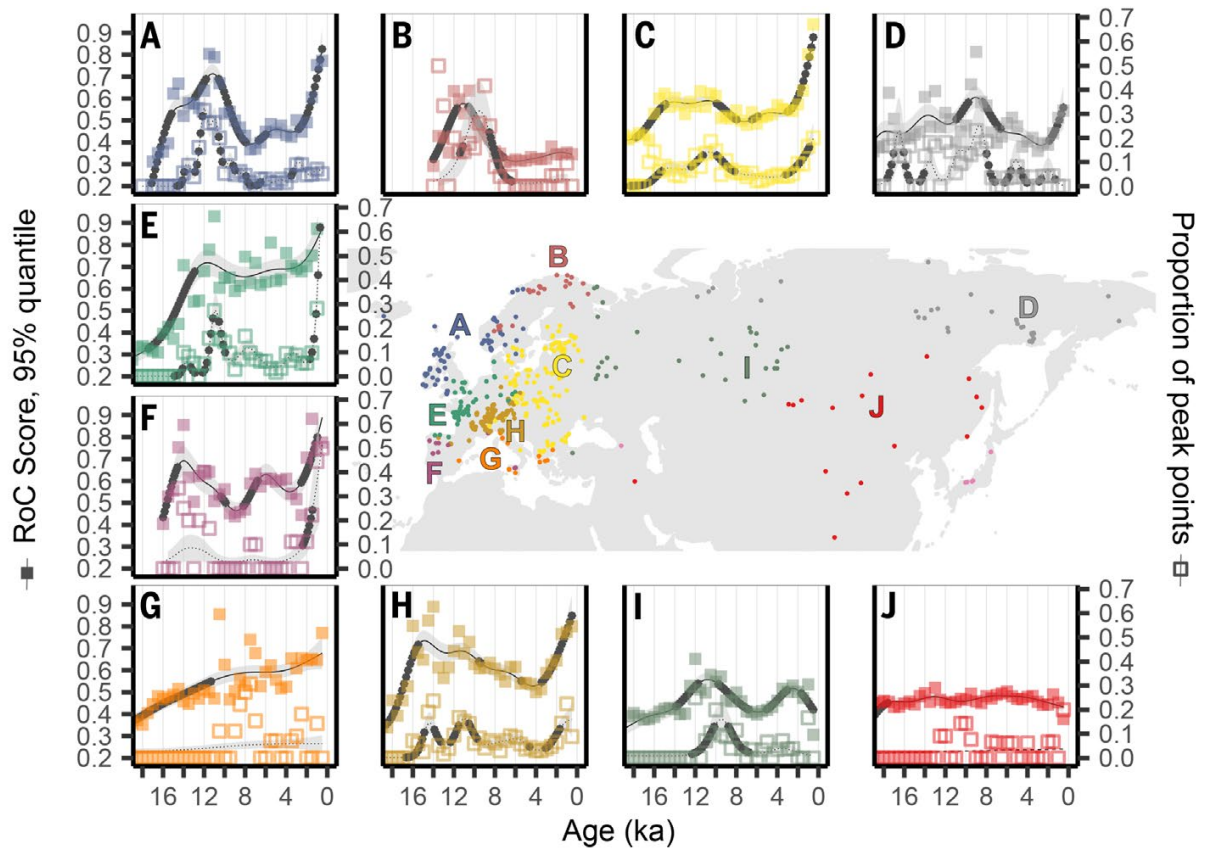
302 sequences (22). When the relationship is not significant, the GAM line is shown as dashed and the

303 error envelope is absent. Black asterisks on the GAM curves identify periods of significant

304 acceleration in vegetation RoCs (i.e. where the derivative significantly differs from zero). Arrows

305 indicate maximum RoC values for late Holocene and the Pleistocene-Holocene transition (**Table S1**).

306



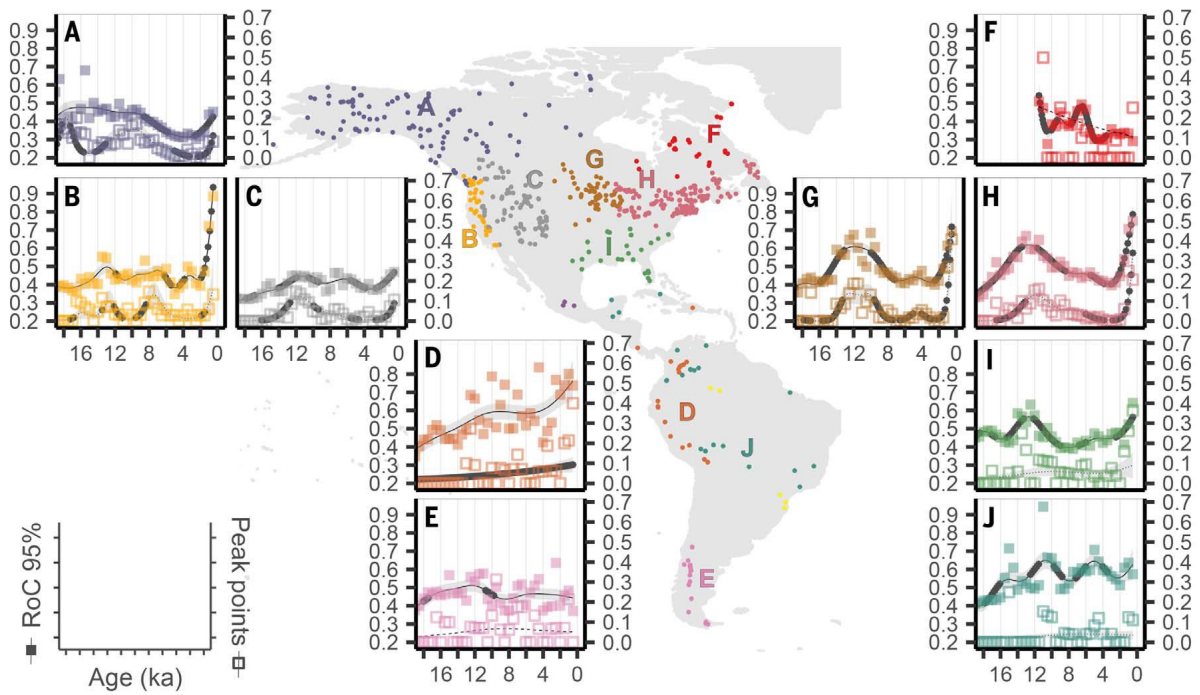
307

308 **Figure 3 | Rates of Change (RoC) analyses by region across Eurasia.** Figure design follows Figure

309 2.

310

311



312

313 **Figure 4 | Rates of Change (RoC) analyses by region across the Americas.** Figure design follows

314 Figure 2.

315

316